



ELSEVIER

Available online at www.sciencedirect.com

Journal of Magnetism and Magnetic Materials 320 (2008) 1961–1965

www.elsevier.com/locate/jmmm

Characterization of magnetic materials by low-field microwave absorption techniques

R. Valenzuela^{a,*}, G. Alvarez^a, H. Montiel^b, M.P. Gutiérrez^c, M.E. Mata-Zamora^b,
F. Barrón^a, A.Y. Sánchez^a, I. Betancourt^a, R. Zamorano^d

^aDepartamento de Materiales Metalicos y Ceramicos, Instituto de Investigaciones en Materiales, Universidad Nacional Autonoma de Mexico, Mexico

^bDepartamento de Tecnociencias, Centro de Ciencias Aplicadas y Desarrollo Tecnologico, Universidad Nacional Autonoma de Mexico, Mexico

^cDepartamento de Química Inorganica y Nuclear, Facultad de Química, Universidad Nacional Autonoma de Mexico, Mexico

^dDepartamento de Ciencia de Materiales, Instituto Politecnico Nacional, Mexico

Available online 13 February 2008

Abstract

A low-field non-resonant microwave absorption has recently been observed in a variety of magnetically ordered materials at low DC fields ($-1000 \text{ Oe} \leq H_{\text{DC}} \leq +1000 \text{ Oe}$), which is known as low-field microwave absorption (LFA). It has been shown that LFA is essentially similar to giant magnetoimpedance (GMI), and clearly different from ferromagnetic resonance (FMR). LFA strongly depends on the anisotropy field of the sample. In contrast with FMR (which can be described as the homogeneous precession of spins in the saturated state), LFA can be thought as a spin rotation process occurring during the magnetic saturation. In this work, we present a detailed study of the basic features of LFA in several types of materials: ferrites and amorphous microwires and ribbons; in particular the effects sample shape, temperature up to the Curie transition, the influence of easy axis and the effects of annealings. These examples show that once LFA is fully understood, it can become a powerful characterization tool.

© 2008 Elsevier B.V. All rights reserved.

PACS: 75.70.Kj; 80.40.-x; 75.60.d

Keywords: Microwave absorption; Ferromagnetic resonance; Curie transition; Anisotropy field

1. Introduction

Microwave absorption at very low magnetic fields has been observed in a wide variety of magnetically ordered materials [1–9]. This absorption is clearly distinct to ferromagnetic resonance (FMR), since it shows hysteresis and is very far from the Larmor conditions. Low field microwave absorption (LFA) has been reported in amorphous thin films [1], amorphous ribbons [2,3,8], glass-coated microwires [4–6], ferrites [7] and multilayers [9]. The general correlation [4,5] of LFA with magnetization processes at low fields was early recognized, and later, the central role of the anisotropy field [1]. Also, in the case of glass-coated microwires, LFA has shown its direct dependence [6] on the mechanical stresses produced by the

glass sheath. The similarity between LFA and giant magnetoimpedance (GMI) has been clearly observed [3,8,9]. In fact, it has been demonstrated [8] that a simple transformation of GMI data (a numerical derivation) leads to the same antisymmetric peak plot typically obtained in LFA.

2. Experimental techniques

Polycrystalline samples of $\text{Ni}_{0.36}\text{Zn}_{0.64}\text{Fe}_2\text{O}_4$ ferrites were prepared by co-precipitation from aqueous solutions of ZnCl_2 , $\text{Fe}(\text{NO}_3)_3 \cdot 9\text{H}_2\text{O}$ and $\text{NiCl}_2 \cdot 6\text{H}_2\text{O}$. An aqueous solution of NaCO_3 was used as a precipitant agent. The chemical reaction was carried out at 60°C for 1 h. The pH was kept at ~ 9 – 11 . The product was sintered at 1000°C for 80 h. X-ray diffraction measurements confirmed a single spinel phase, with a unit cell parameter of 0.8408 nm . The Curie temperature, $T_C = 425 \pm 5 \text{ K}$, was determined by

*Corresponding author.

E-mail address: monjaras@servidor.unam.mx (R. Valenzuela).

means of the thermal variations of the initial permeability [10], on toroidally shaped samples.

As-spun, glass-coated amorphous microwires of compositions $\text{Co}_{69.4}\text{Fe}_{3.7}\text{B}_{15.9}\text{Si}_{11}$ and $\text{Fe}_{74}\text{B}_{11}\text{Si}_{15}$, prepared by the Taylor–Ulitoski technique, were also used for measurements. The metal diameter was $24\ \mu\text{m}$ with a total diameter (metal + glass) of $30\ \mu\text{m}$ for the CoFe microwires, and $24\ \mu\text{m}$ and $32\ \mu\text{m}$ for the Fe microwires, respectively.

We also investigated amorphous ribbons of nominal composition $\text{Co}_{66}\text{Fe}_4\text{B}_{12}\text{Si}_{13}\text{Nb}_4\text{Cu}$, prepared by melt-spinning at a tangential speed of 30 m/s. They were subjected to thermal annealings of 5, 10 and 20 min at 723 K, in an inert atmosphere. Microwave measurements were carried out on small pieces $\sim 1\ \text{mm}$ wide and $\sim 2\ \text{mm}$ length, with the ribbon axis parallel to the DC applied field.

The low magnetic field section of ferromagnetic absorption of samples, or LFA measurements were performed using a Jeol JES-RES3X spectrometer operating at 9.4 GHz (X-band). The power of the ac signal was 1 mW. A Jeol ES-ZCS2 zero-cross sweep unit was used to digitally compensate for any remanence in the electromagnet, thus allowing measurements to be carried out by cycling the DC magnetic field about its zero value continuously from -1 to $1\ \text{kOe}$, with a standard deviation of less than $0.2\ \text{Oe}$ for the measured field. The FMR of the samples was also determined. All microwave measurements for ferrite samples were carried out in the 100–450 K temperature range. For amorphous microwires, microwave measurements were performed at room temperature on microwire pieces 2 mm length. The angle between the ribbon longitudinal axis and the DC field direction was varied by 180° , both by keeping the DC in the ribbon plane, and by measuring with the DC field through a normal direction to the ribbon plane.

3. Results and discussion

Fig. 1 shows the resonant microwave absorption spectra $[dP/dH=f(H_{\text{dc}})]$ of Ni–Zn ferrite at a few selected temperatures. A single broad line is observed in the whole temperature range, with a shift in resonant field H_{res} and a decrease in linewidth as T increases. The asymmetric FMR signal changes gradually to a symmetric electron paramagnetic resonance (EPR) signal as the Curie temperature is reached. The resonance condition is expressed [11] as $\omega = \gamma H_{\text{res}}$, where ω is the angular frequency ($\omega = 2\pi f$), γ is the gyromagnetic ratio ($\gamma = eg_{\text{eff}}/2m$), and H_{res} is the total field, i.e., $H_{\text{res}} = H_{\text{dc}} - H_i$, where H_i is the effective internal field, which includes all the contributions associated with the ordered structure (anisotropy, superexchange, etc.). In the ferrimagnetic ordered phase the internal field adds to the applied field and the resonance condition is reached at low values of H_{dc} ; in contrast, in the paramagnetic, disordered region, $H_i = 0$ and $H_{\text{res}} = H_{\text{dc}}$. This explains the shift H_{dc} as the Curie temperature is attained.

The temperature dependence of the total linewidth ΔH_{pp} is plotted in Fig. 2. ΔH_{pp} decreases because H_i weakens

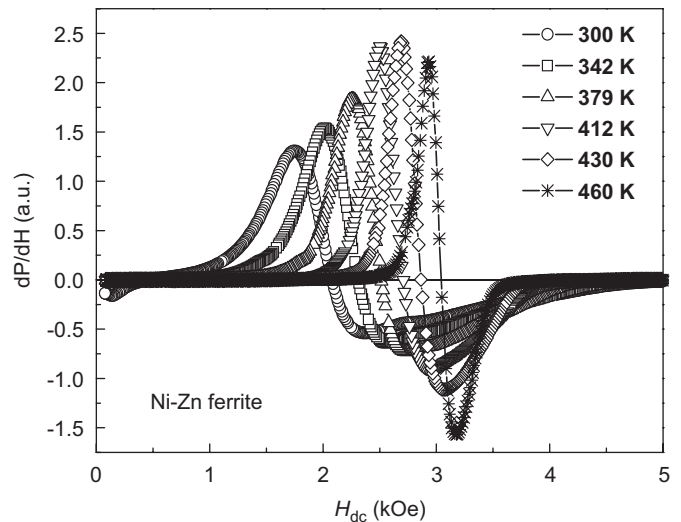


Fig. 1. Resonant microwave absorption spectra of Ni–Zn ferrite for selected temperatures in the 300–460 K range.

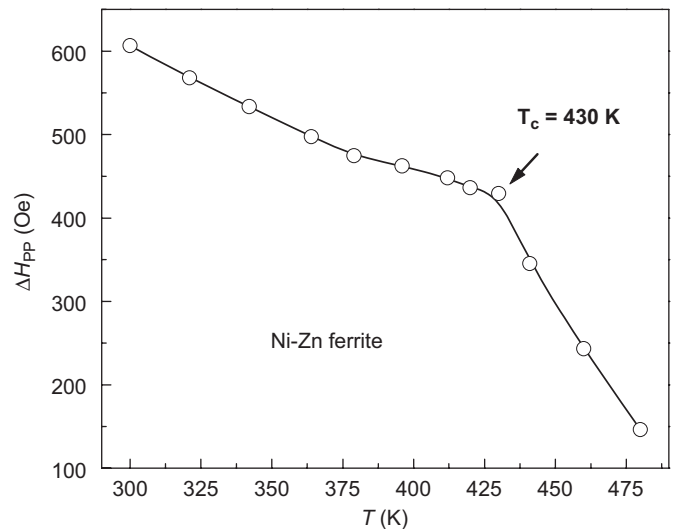


Fig. 2. Temperature dependence of the total linewidth from 300 to 480 K. The line connecting points is only a guide for the eye.

(both superexchange and anisotropy decrease as a result of increased thermal vibrations) as the transition is approached. A change of slope is observed at $T = 430\ \text{K}$, which agrees very well with the value measured for these samples by means of the thermal variations in initial magnetic permeability [10].

Once the magnetic transition has been established, we turn to LFA results for some selected temperatures, as shown in Fig. 3. These results correspond to the low-field section of the same plot, but here the plot is enlarged, and includes the $-1\ \text{kOe} \leq H_{\text{dc}} \leq +1\ \text{kOe}$ field range. The signal exhibits two antisymmetric peaks, with some hysteresis as the field is cycled. The peak-to-peak value (the difference in magnetic field between maxima and minima peaks), ΔH_{LFA} , decreases with T and disappears at $T \sim 430\ \text{K}$. We can therefore state that LFA is strongly associated with magnetization processes of the ordered phase. The presence

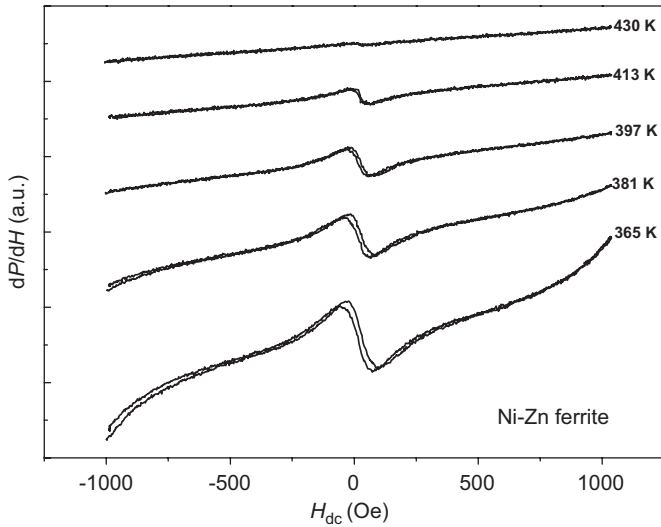


Fig. 3. LFA spectra for selected temperatures in the 300–430 K range.

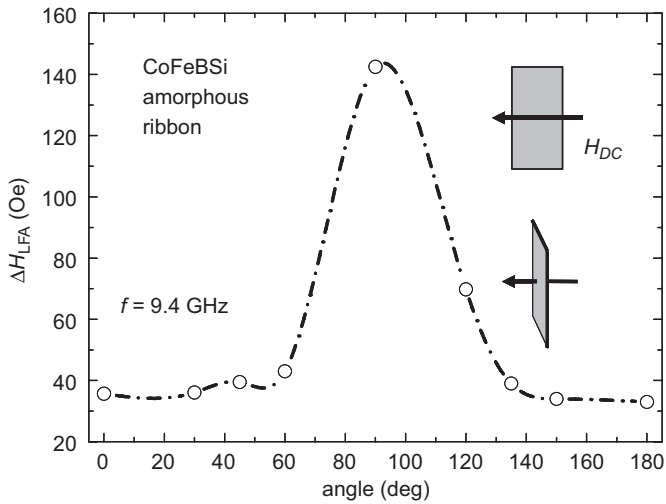


Fig. 4. LFA plot of Co-rich amorphous ribbons by varying the angle between the ribbon plane and the direction of the DC field, as shown in inset.

of hysteresis, as well as the fact that the absorption conditions are very different from FMR (as explained in the above paragraph) allows us to state that LFA is a non-resonant phenomenon.

The shape of the sample plays an important role on LFA. Measurements of LFA in Co-rich amorphous ribbons by varying the angle between the ribbon plane and the DC field led to drastic changes [12], where the peak-to-peak field increased as a function of angle between 0° and 90°, while the amplitude decreased, as shown in Fig. 4. Clearly, this is the effect of shape anisotropy. The less-pronounced changes in LFA (but no less significant) were observed also by varying the angle between the DC field and the ribbon longitudinal axis, keeping always the field within the ribbon plane (Fig. 5). Here, two minima are observed: one in the parallel orientation, and one

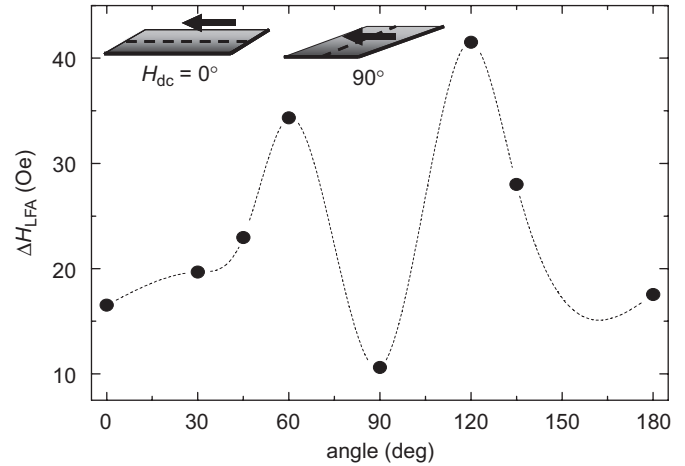


Fig. 5. LFA plots of Co-rich amorphous ribbons by varying the angle between the ribbon axis and the DC field, and keeping the field within the ribbon plane, as shown in inset.

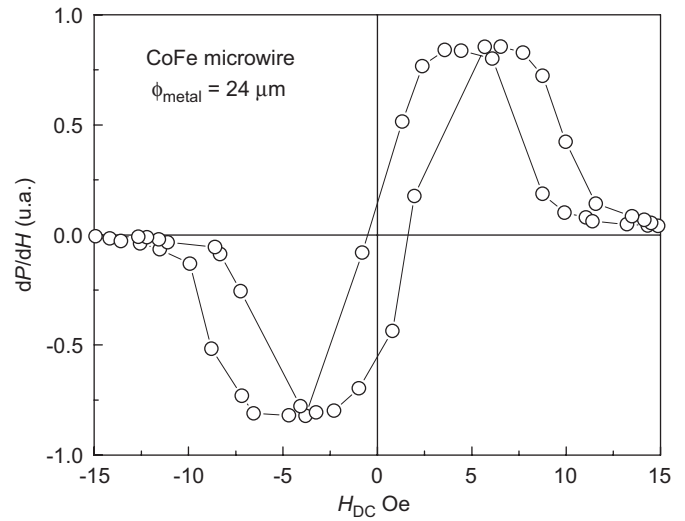


Fig. 6. LFA spectrum of CoFe amorphous microwires.

perpendicular to the ribbon axis, respectively. Since these ribbons possess a small negative magnetostriction, the magnetization tends to be oriented perpendicular to the ribbon axis, which explains the perpendicular minimum. However, shape anisotropy is always present, and the overall result is a combination of both induced and shape anisotropies.

LFA in CoFe and Fe amorphous microwires have also been measured, as shown in Figs. 6 and 7, respectively. A comparison of these results provides more insight into LFA. Here, measurements were carried out by placing the microwires axis parallel to the DC magnetic field (and perpendicular to the AC field). For a Co/Fe ratio of about ~16 (~94/6), CoFe microwires show a very small and negative magnetostriction, which leads to a magnetic domain structure of “core and shell”; the core is magnetized parallel to the wire axis, and the shell exhibits

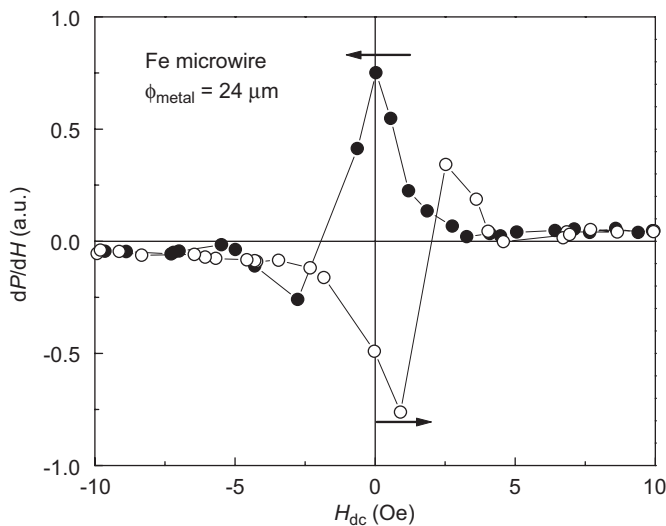


Fig. 7. LFA spectra of Fe amorphous microwires.

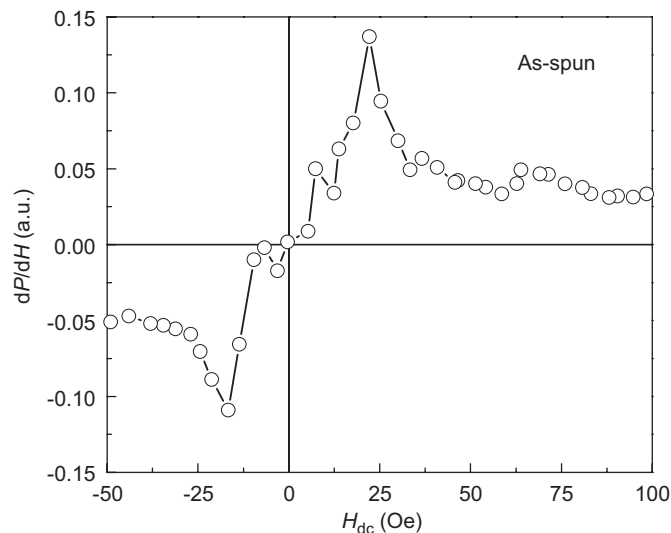


Fig. 8. LFA plot of the as-spun amorphous ribbon, in the -50 to $+100$ Oe field range.

a circumferential easy-axis. As a DC magnetic field is applied in the wire axis, most of magnetization changes occur by domain rotation instead of domain wall movements, since circumferential domains are oriented perpendicular to the DC field. Rounded maxima and minima are therefore observed in LFA, as shown in Fig. 6.

Fe-rich amorphous alloys possess a positive saturation magnetostriction and the easy axis is therefore oriented parallel to the wire axis. Since the easy axis is parallel to the DC field, magnetization processes (produced by the DC field) proceed essentially by domain wall displacements. In fact, these microwires exhibit a “bistable” behavior [13]; the application of an axial field opposite to axial domains leads to the nucleation of a domain wall oriented in the field direction, which moves very rapidly by a large Barkhausen jump (LBJ). This accounts for the observed geometry of LFA, where narrow, asymmetric peaks are observed, with a considerable hysteresis, Fig. 7.

We now consider the effects of thermal annealings on amorphous ribbons of nominal composition $\text{Co}_{66}\text{Fe}_4\text{B}_{12}\text{Si}_{13}\text{Nb}_4\text{Cu}$, prepared by melt-spinning, as observed by means of LFA. In all the following plots, the magnetic field was applied from the negative value (-50 Oe) up to $+100$ Oe. Fig. 8 shows the LFA of the as-spun ribbon. Some random variations appear in most of the plots, and especially in the inversion of dP/dH values, which can be attributed to the residual stresses after the rapid cooling. The difference in magnetic field between the minimum and the maximum is $\Delta H_{\text{LFA}} \sim 39$ Oe, i.e., the anisotropy field is about 19 Oe, which is in good agreement with impedance measurements at high frequencies. After 5 min of annealing, the plot has become a little smoother, and the LFA field has increased to $\Delta H_{\text{LFA}} \sim 43$ Oe as appears in Fig. 9. The smoothing of the curve can then be interpreted in terms of the beginning of structural relaxation. A strong change can be observed for an annealing time of 10 min (Fig. 10); the inversion is very narrow and occurs

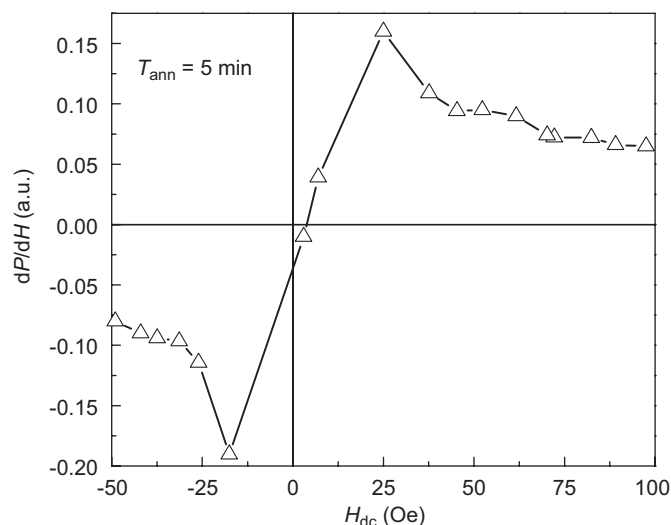


Fig. 9. LFA of amorphous ribbons annealed during 5 min at 723 K.

within ~ 8 Oe. This indicates that nanocrystallization has occurred, and the anisotropy field has decreased ~ 5 times. Finally, Fig. 11 shows the effects of annealing for 20 min. The inversion encompasses 41 Oe, and we can consider that magnetic hardening, presumably by crystallite growth, has started.

To our knowledge, the mechanisms of LFA signal, which involves the microwave absorption from the unsaturated state at zero applied field, are not fully explained. However, a schematic description could be as follows. At zero DC field, the microwave absorption by the spins is strongly damped since they have a random distribution. As the DC field increases, the domains oriented closer to the field direction grow at the expense of the domains oriented against this direction, and some microwave absorption can take place due to this

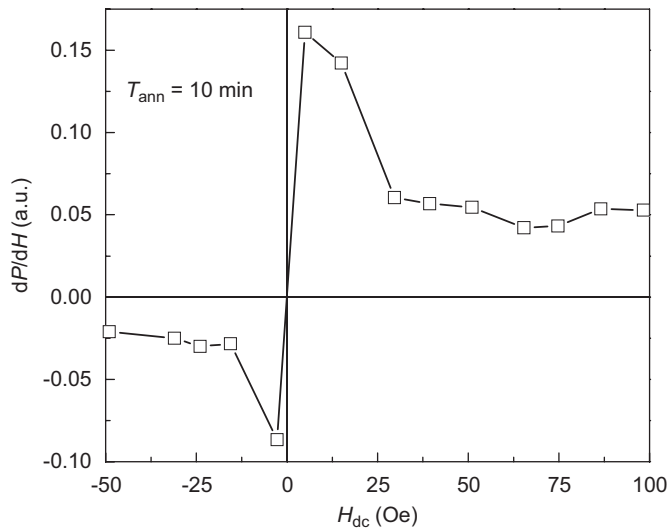


Fig. 10. LFA of amorphous ribbons annealed during 10 min at 723 K. A large softening is appeared as the LFA field $\Delta H_{LFA} \sim 8$ Oe.

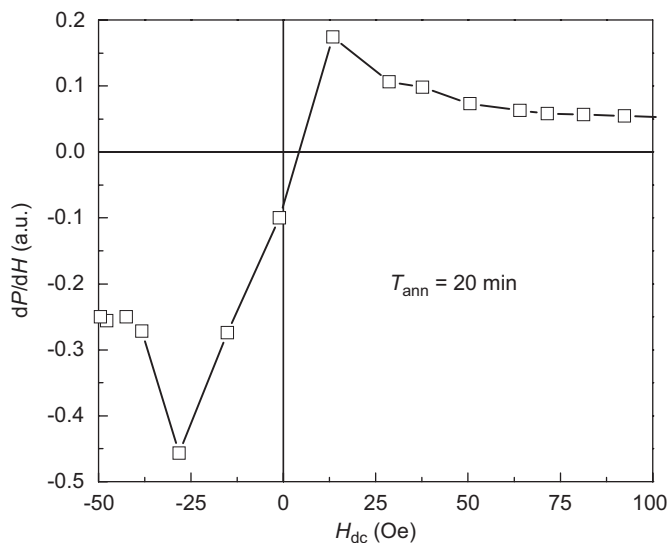


Fig. 11. LFA of the sample annealed 20 min, leading to $\Delta H_{LFA} \sim 8$ Oe.

unbalanced domain structure. Domain walls move as a result of the DC field variations; the frequency of AC field, in the tens of GHz, is too high for them to follow it. The spin dynamics is therefore associated with spin rotation in an unsaturated state. As the DC field reaches the anisotropy field value, spin rotation goes through a maximum because the DC field has finally overcome

anisotropy; accordingly, LFA signal shows a maximum. A very good agreement between the difference in magnetic field between maxima and minima direction, and some microwave absorption can take place due to this unbalanced domain structure. Domain walls move as a result of the DC field variations; the frequency of AC field, in the tens of GHz, is too high for them to follow it.

4. Conclusions

We have shown the application of LFA experiments in several interesting cases in ferri and ferromagnetic materials. It appears that LFA is strongly dependent on magnetization processes; in fact LFA seems directly associated with the spin rotation absorption driven by the AC field, in the unsaturated sample. LFA can become an excellent characterization technique due to its sensitivity and flexibility of application.

Acknowledgment

G. Alvarez acknowledges a postdoctoral fellowship from CONACYT-Mexico.

References

- [1] M. Rivoire, G. Suran, *J. Appl. Phys.* 78 (1995) 1899.
- [2] A.N. Medina, M. Knobel, S. Salem-Sugui, F.G. Gandra, *J. Appl. Phys.* 79 (1999) 5462.
- [3] H. Montiel, G. Alvarez, I. Betancourt, R. Zamorano, R. Valenzuela, *Appl. Phys. Lett.* 86 (2005) 072503.
- [4] H. Chiriac, C.N. Colesniuc, T.-A. Ovari, M. Ticusan, *J. Appl. Phys.* 85 (1999) 5453.
- [5] H. Chiriac, C.N. Colesniuc, T.-A. Ovari, *J. Magn. Magn. Mater.* 215–216 (2000) 407.
- [6] H. Montiel, G. Alvarez, M.P. Gutiérrez, R. Zamorano, R. Valenzuela, *IEEE Trans. Magn.* 41 (2006) 3380.
- [7] H. Montiel, G. Alvarez, M.P. Gutiérrez, R. Zamorano, R. Valenzuela, *J. Alloys Compd.* 369 (2004) 141.
- [8] G. Alvarez, H. Montiel, D. de Cos, R. Zamorano, A. García-Arribas, J.M. Barandiarán, R. Valenzuela, *J. Non-Cryst. Solids* 353 (2007) 902.
- [9] D. de Cos, A. García-Arribas, G. Alvarez, H. Montiel, R. Zamorano, J.M. Barandiarán, R. Valenzuela, *Sens. Lett.* 5 (2007) 73.
- [10] E. Cedillo, J. Ocampo, V. Rivera, R. Valenzuela, *J. Phys. E: Sci. Instrum.* 13 (1980) 383.
- [11] A.H. Morrish, *The Physical Principles of Magnetism*, Wiley, New York, 1965.
- [12] H. Montiel, G. Alvarez, R. Zamorano, R. Valenzuela, *J. Non-Cryst. Solids* 353 (2007) 908.
- [13] A.P. Chen, A. Zhukov, J. Gonzalez, L. Dominguez, J.M. Blanco, *J. Appl. Phys.* 100 (2006) 083907.